Timing Belt Theory

Timing Belt Theory

Introduction

This paper presents a thorough explanation of geometric, loading and deflection relationships of reinforced urethane timing belts. It covers valuable background for the step by step selection procedure for the "Belt Sizing Guide" available on the Gates Mectrol web site. Traditional understanding of timing belt drives comes from power transmission applications. However, the loading conditions on the belt differ considerably between power transmission applications and conveying and linear positioning applications. This paper presents analysis of conveying and linear positioning applications. Where enlightening, reference will be made to power transmission and rotary positioning drives. For simplicity, only two pulley arrangements are considered here; however, the presented theory can be extended to more complex systems.

Geometric Relationships

Belt and Pulley Pitch

Belt pitch, ***p***, is defined as the distance between the centerlines of two adjacent teeth and is measured at the belt pitch line (Fig. 1). The *belt pitch line* is identical to the neutral bending axis of the belt and coincides with the center line of the cords.

Pulley pitch is measured on the *pitch circle* and is defined as the arc length between the centerlines of two adjacent pulley grooves (Figs. 1a and 1b). The *pitch circle* coincides with the pitch line of the belt while wrapped around the pulley. In timing belt drives the pulley *pitch diameter*, ***d***, is larger than the pulley

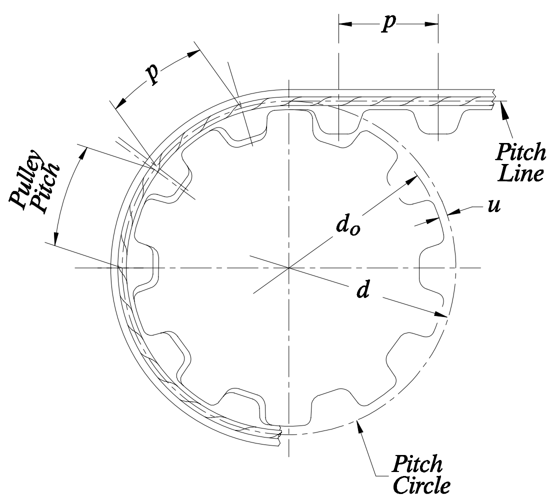

Figure 1a. Belt and pulley mesh for inch series and metric T-series, HTD and STD series geometry.

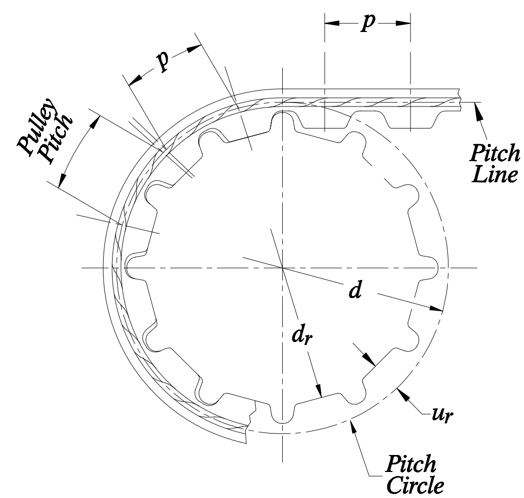

Figure 1b. Belt and pulley mesh for AT-series geometry.

outside diameter, $\boldsymbol{d_o}$. The pulley pitch diameter is given by

$$d = \frac{p \cdot z_p}{\pi} \quad (1)$$

where p is the *nominal pitch* and $\boldsymbol{z_p}$ the *number of pulley teeth*.

The radial distance between pitch diameter and pulley outer diameter is called *pitch differential*, $\boldsymbol{u}$, and has a standard value for a given belt section of *inch pitch* and *metric T series* belts (see Table 1). The pulley outside diameter can be expressed by

$$d_o = d - 2u = \frac{p \cdot z_p}{\pi} - 2u \quad (2)$$

As inch pitch and metric T series belts are designed to ride on the top lands of pulley teeth, the tolerance of the outside pulley diameter may cause the pulley pitch to differ from the nominal pitch (see Fig. 1a).

On the other hand, metric AT series belts are designed to contact bottom lands (not the top lands) of a pulley as shown in Fig. 1b. Therefore, pulley pitch and pitch diameter are affected by tolerance of the pulley *root diameter*, $\boldsymbol{d_r}$, which can be expressed by

$$d_r = d - 2u_r = \frac{p \cdot z_p}{\pi} - 2u_r \quad (3)$$

The radial distance between pitch diameter

Belt section		***p*** *- belt pitch*	***H*** *- belt height*	***u*** *- pitch differential*	***h*** *- tooth height*
XL	in	0.200	0.090	0.010	0.050
	mm	5.1	2.3	0.3	1.3
L	in	0.375	0.140	0.015	0.075
	mm	9.5	3.6	0.4	1.9
H	in	0.500	0.160	0.027	0.090
	mm	12.7	4.1	0.7	2.3
XH	in	0.875	0.440	0.055	0.250
	mm	22.2	11.2	1.4	6.4
T5	in	0.197	0.087	0.020	0.047
	mm	5.0	2.2	0.5	1.2
T10	in	0.394	0.177	0.039	0.098
	mm	10.0	4.5	1.0	2.5
T20	in	0.787	0.315	0.059	1.500
	mm	20.0	8.0	1.5	5.0
HTD 5	in	0.197	0.142	0.028	0.83
	mm	5.0	3.6	0.7	2.1
HTD 8	in	0.315	0.220	0.028	0.134
	mm	8.0	5.6	0.7	3.4
HTD 14	in	0.551	0.394	0.055	0.236
	mm	14.0	10.0	1.4	6.0
STD 5	in	0.197	0.134	0.028	0.075
	mm	5.0	3.4	0.7	1.9
STD 8	in	0.315	0.205	0.028	0.11
	mm	8.0	5.2	0.7	3.0
STD 14	in	0.551	0.402	0.055	0.209
	mm	14.0	10.2	1.4	5.3

Table 1

Belt section	***p*** *- belt pitch*	***H*** *- belt height*	***u***	***h*** *- tooth height*
AT5 in	0.197	0.106	0.077	0.047
mm	5.0	2.7	2.0	1.2
AT10 in	0.394	0.177	0.138	0.098
mm	10.0	4.5	3.5	2.5
AT20 in	0.787	0.315	0.256	0.197
mm	20.0	8.0	6.5	5.0

Table 2

and root diameter, $\boldsymbol{u_r}$, has a standard value for a particular AT series belt sections (see Table 2).

Belt Length and Center Distance

Belt length, ***L***, is measured along the pitch line and must equal a whole number of belt pitches (belt teeth), $\boldsymbol{z_b}$

$$L = p \cdot z_b \tag{4}$$

Most linear actuators and conveyors are designed with two equal diameter pulleys. The relationship between belt length, ***L***, *center distance*, ***C***, and pitch diameter, ***d***, is given by

$$L = 2 \cdot C + \pi \cdot d \tag{5}$$

For drives with two unequal pulley diameters (Fig. 2) the following relationships can be written:

Angle of wrap, $\boldsymbol{\theta_1}$, around the small pulley

$$\theta_1 = 2\arccos\left(\frac{d_2 - d_1}{2 \cdot C}\right) \tag{6}$$

where $\boldsymbol{d_1}$ and $\boldsymbol{d_2}$ are the pitch diameters of the small and the large pulley, respectively.

Angle of wrap, $\boldsymbol{\theta_2}$, around the large pulley

$$\theta_2 = 2 \cdot \pi - \theta_1 \tag{7}$$

Span length, $\boldsymbol{L_s}$

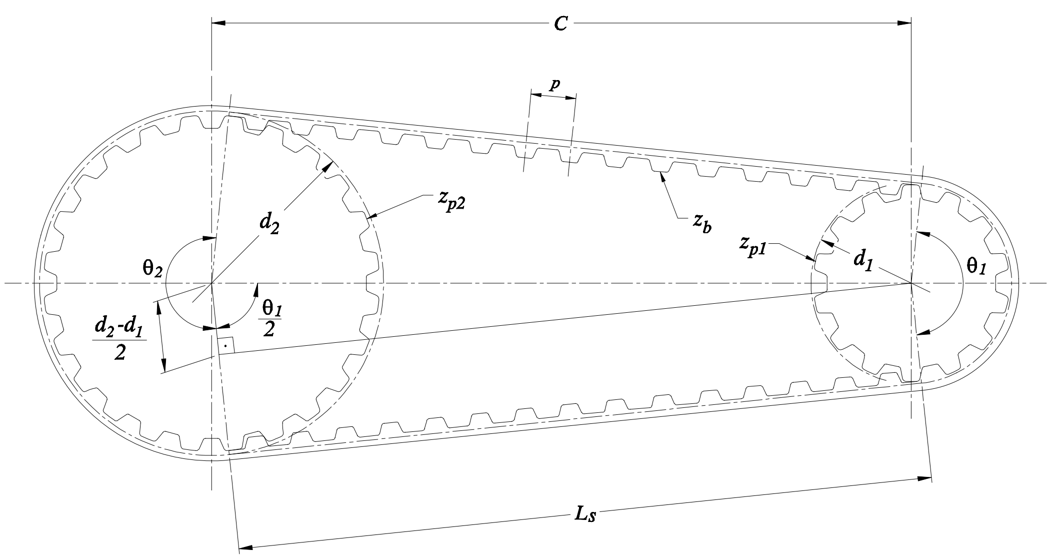

Figure 2. Belt drive with unequal pulley diameters.

$$L_s = C \cdot \sin\left(\frac{\theta_1}{2}\right) \quad (8)$$

Belt length, ***L***

$$L = 2 \cdot C \cdot \sin\left(\frac{\theta_1}{2}\right) + \theta_1 \cdot \frac{d_1}{2} + \left(2 \cdot \pi - \theta_1\right) \cdot \frac{d_2}{2} \quad (9)$$

Since angle of wrap, $\boldsymbol{\theta_1}$, is a function of the center distance, ***C***, Eq. (9) does not have a closed form solution for ***C***. It can be solved using any of available numerical methods.
An approximation of the center distance as a function of the belt length is given by

$$C \approx \frac{Y + \sqrt{Y^2 - 2 \cdot \left(d_2 - d_1\right)^2}}{4} \quad (10)$$

where $Y = L - \frac{\pi \cdot \left(d_2 + d_1\right)}{2}$

Forces Acting in Timing Belt Drives

A timing belt transmits torque and motion from a driving to a driven pulley of a power transmission drive (Fig. 3), or a force to a positioning platform of a linear actuator (Fig. 4). In conveyors it may also carry a load placed on its surface (Fig. 6).

Torque, Effective Tension, Tight and Slack Side Tension

During operation of belt drive under load a difference in belt tensions on the entering (tight) and leaving (slack) sides of the driver pulley is developed. It is called *effective tension*, $\boldsymbol{T_e}$, and represents the force transmitted from the *driver* pulley to the belt

$$T_e = T_1 - T_2 \quad (11)$$

where $\boldsymbol{T_1}$ and $\boldsymbol{T_2}$ are the *tight* and *slack side tensions*, respectively.

The driving torque, ***M*** ($\boldsymbol{M_1}$ in Fig. 3), is given by

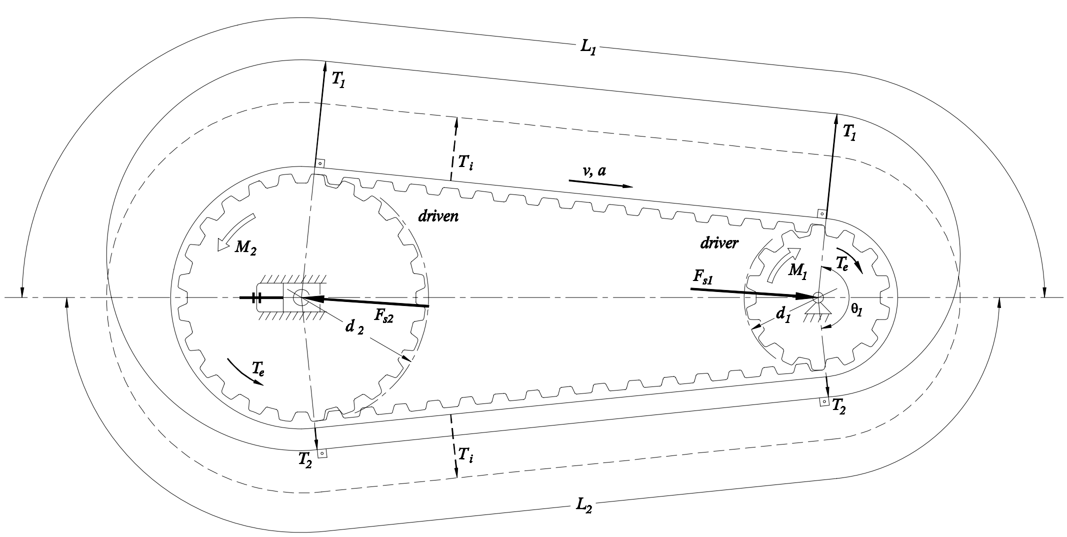

Figure 3. Power transmission and rotary positioning.

$$M = T_e \cdot \frac{d}{2} \qquad (12)$$

where d (d_1 in Fig. 3) is the pitch diameter of the driver pulley.
The effective tension generated at the driver pulley is the actual working force that overcomes the overall resistance to the belt motion. It is necessary to identify and quantify the sum of the individual forces acting on the belt that contribute to the effective tension required at the driver pulley.

In *power transmission* drives (Fig. 3), the resistance to the motion occurs at the driven pulley. The force transmitted from the belt to the *driven* pulley is equal to T_e. The following expressions for torque requirement at the driver can be written

$$M_1 = T_e \cdot \frac{d_1}{2} = \frac{M_2}{\eta} \cdot \frac{d_1}{d_2} = \frac{P_2 \cdot d_1}{\omega_2 \cdot \eta \cdot d_2} = \frac{P_2}{\omega_1 \cdot \eta} \qquad (13)$$

where M_1 is the driving torque, M_2 is the torque requirement at the driven pulley, P_2 is the power requirement at the driven pulley, ω_1 and ω_2 are the angular speeds of the driver and driven pulley respectively, d_1 and d_2 are the pitch diameters of the driver and driven pulley respectively, and η is the efficiency of the belt drives ($\eta = 0.94 - 0.96$ typically). The angular speeds of the driver and driven pulley ω_1 and ω_2 are related in a following form:

$$\omega_2 = \omega_1 \cdot \frac{d_1}{d_2} \qquad (14)$$

The relationship between the angular speeds and rotational speeds is given by

$$\omega_{1,2} = \frac{\pi \cdot n_{1,2}}{30} \qquad (15)$$

where n_1 and n_2 are rotational speeds of the driver and driven pulley in revolutions per minute [rpm], and ω_1 and ω_2 are angular velocities of the driver and driven pulley in radians per second.

In *linear positioners* (Fig. 4) the main load acts at the positioning platform (slider). It consists of acceleration force F_a (linear acceleration of the slider), friction force of the linear bearing, F_f, external force (work

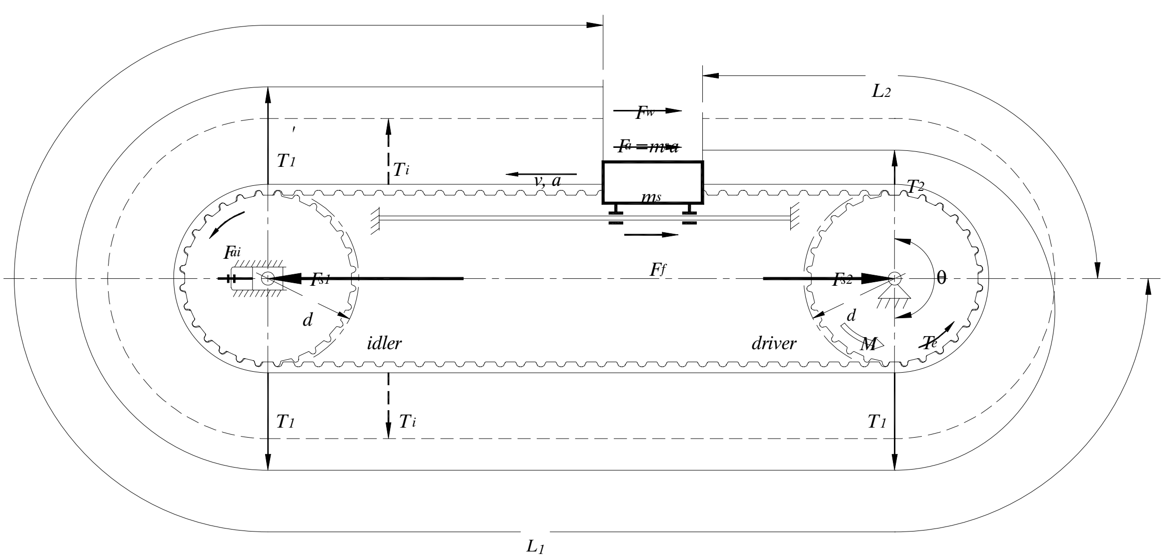

Figure 4. Linear positioner - configuration I.

load), $\boldsymbol{F_w}$, component of weight of the slide $\boldsymbol{F_g}$ parallel to the belt in inclined drives, inertial forces to accelerate belt, $\boldsymbol{F_{ab}}$, and the idler pulley, $\boldsymbol{F_{ai}}$ (rotation)

$$T_e = F_a + F_f + F_w + F_g + F_{ab} + F_{ai} \quad (16)$$

The individual components of the effective tension, $\boldsymbol{T_e}$, are given by

$$F_a = m_s \cdot a \quad (17)$$

where $\boldsymbol{m_s}$ is the mass of the slider or platform and $\boldsymbol{a}$ is the linear acceleration rate of the slider,

$$F_f = \mu_r \cdot m_s \cdot g \cdot \cos\beta + F_{fi} \quad (18)$$

where $\boldsymbol{\mu_r}$ is the dynamic coefficient of friction of the linear bearing (usually available from the linear bearing manufacturer), $\boldsymbol{F_{fi}}$ is a load independent resistance intrinsic to linear motion (seal drag, preload resistance, viscous resistance of the lubricant, etc.) and $\boldsymbol{\beta}$ is the angle of incline of the linear positioner,

$$F_g = m_s \cdot g \cdot \sin\beta \quad (19)$$

$$F_{ab} = \frac{w_b \cdot L \cdot b}{g} \cdot a \quad (20)$$

where $\boldsymbol{L}$ is the length of the belt, $\boldsymbol{b}$ is the width of the belt, $\boldsymbol{w_b}$ is the specific weight of the belt and $\boldsymbol{g}$ is the gravity,

$$F_{ai} = \frac{2 \cdot J_i \cdot \alpha}{d} = \frac{m_i}{2} \cdot \left(1 + \frac{d_b^2}{d^2}\right) \cdot a \quad (21)$$

where $\boldsymbol{J_i}$ is the inertia of the idler pulley, $\boldsymbol{\alpha}$ is the angular acceleration of the idler, $\boldsymbol{m_i}$ is the mass of the idler, $\boldsymbol{d}$ is the diameter of the idler and $\boldsymbol{d_b}$ is the diameter of the idler bore (if applicable).

An alternate linear positioner arrangement is shown in Fig. 5. This drive, the slide houses the driver pulley and two idler rolls that roll on the back of the belt. The slider moves along the belt that has both ends clamped in stationary fixtures.

Similar to the linear positioning drive such as configuration I" the effective tension is comprised of linear acceleration force $\boldsymbol{F_a}$, friction force of the linear bearing, $\boldsymbol{F_f}$, external force (work load), $\boldsymbol{F_w}$, component of weight of the slide $\boldsymbol{F_g}$ parallel to the belt in inclined drives and inertial force to accelerate the idler pulleys, $\boldsymbol{F_{ai}}$ (rotation)

$$T_e = F_a + F_f + F_w + F_g + 2 \cdot F_{ai} \quad (22)$$

The individual components of the effective tension, $\boldsymbol{T_e}$, are given by

$$F_a = \left(m_s + m_p + 2 \cdot m_i\right) \cdot a \quad (23)$$

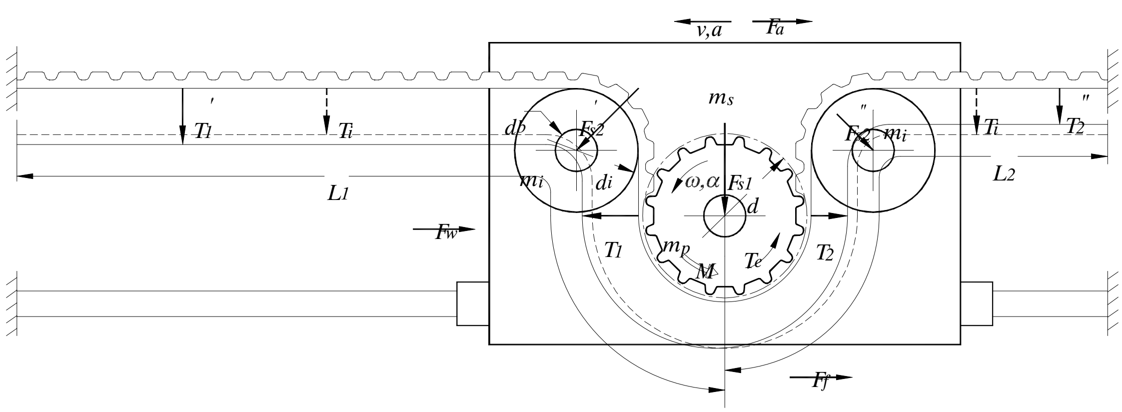

Figure 5. Linear positioner - configuration II.

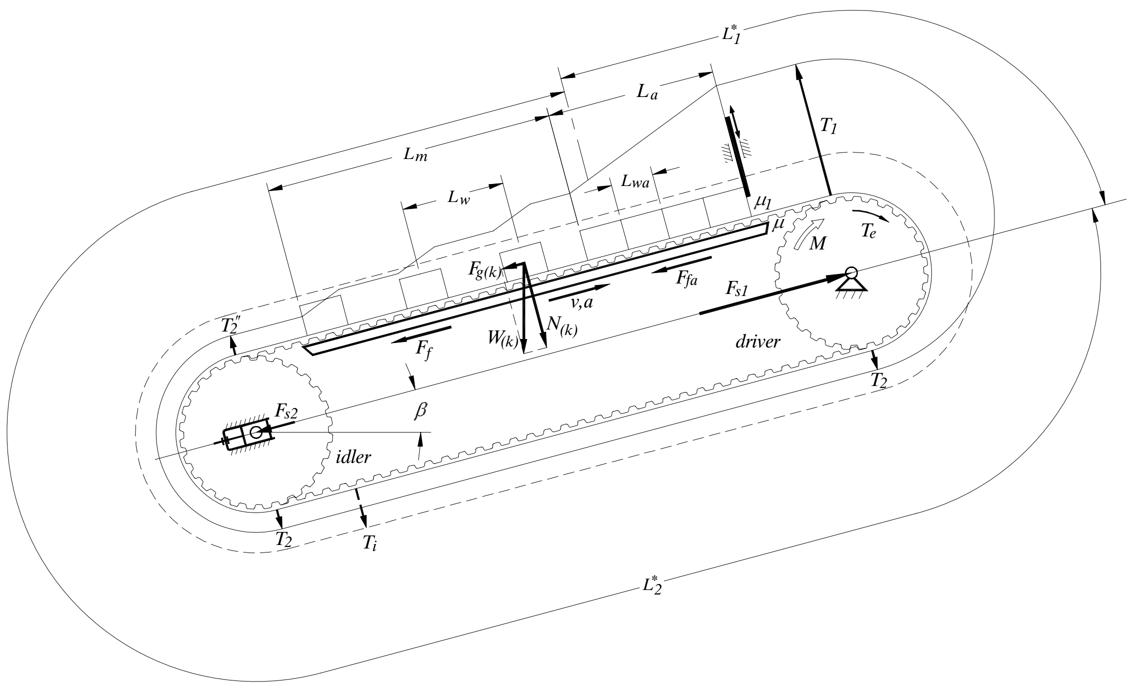

Figure 6. Inclined conveyor with material accumulation.

where $\boldsymbol{m_s}$ is the mass of the slider or platform, $\boldsymbol{m_p}$ is the mass of the driver pulley, $\boldsymbol{m_i}$ is the mass of the idler rollers and $\boldsymbol{a}$ is the translational acceleration rate of the slider,

$$F_f = \mu_r \left(m_s + m_p + 2m_i \right) \cdot g \cdot \cos\beta + F_{fi} \tag{24}$$

where $\boldsymbol{\mu_r}$ is the dynamic coefficient of friction of the linear bearing, $\boldsymbol{F_{fi}}$ is a load independent resistance intrinsic to linear motion and $\boldsymbol{\beta}$ is the angle of incline of the linear positioner,

$$F_g = \left(m_s + m_p + 2 \cdot m_i \right) \cdot g \cdot \sin\beta \tag{25}$$

where $\boldsymbol{\beta}$ is the angle of incline of the linear positioner,

$$F_{ai} = 2 \cdot \frac{2 \cdot J_i \cdot \alpha}{d} = m_i \cdot \left(1 + \frac{d_b^2}{d_i^2} \right) \cdot a \tag{26}$$

where $\boldsymbol{J_i}$ is the inertia of the idler pulley reflected to the driver pulley, $\boldsymbol{\alpha}$ is the angular acceleration of the driver pulley, $\boldsymbol{m_i}$ is the mass of the idler, $\boldsymbol{d}$ is the diameter of the driver, $\boldsymbol{d_i}$ is the diameter of the idler and $\boldsymbol{d_b}$ is the diameter of the idler bore (if applicable).

In inclined *conveyors* in Fig. 6, the effective tension has mainly two forces to overcome: friction and gravitational forces. The component of the friction force due to the conveyed load, $\boldsymbol{F_f}$, is given by

$$F_f = \mu \cdot \sum_{k=1}^{n_c} N_{(k)} = \mu \cdot \cos\beta \cdot \sum_{k=1}^{n_c} W_{(k)} \tag{27}$$

where $\boldsymbol{\mu}$ is the friction coefficient between the belt and the slider bed, $\boldsymbol{N_{(k)}}$ is a component of weight, $\boldsymbol{W_{(k)}}$, of a single conveyed package perpendicular to the belt, $\boldsymbol{n_c}$ is the number of packages being conveyed, index $\boldsymbol{k}$ designates the kth piece of material along the belt and $\boldsymbol{\beta}$ is the angle of incline. When conveying granular materials the friction force is given by

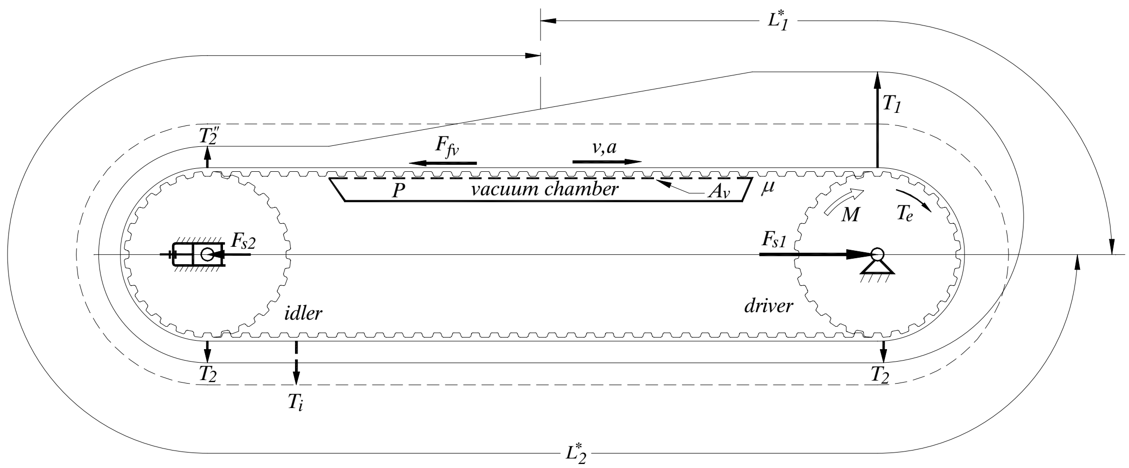

Figure 7. Vacuum conveyor.

$$F_f = \mu \cdot w_m \cdot L_m \cos\beta \tag{28}$$

where $\boldsymbol{w_m}$ is weight distribution over a unit of conveying length and $\boldsymbol{L_m}$ is the conveying length.

Some conveying applications include material accumulation (see Fig. 6). Here an additional friction component due to the material sliding on the back surface of the belt is present and is given by

$$\begin{aligned} F_{fa} &= (\mu + \mu_1) \cdot \sum_{k=1}^{n_a} N_{(k)} \\ &= (\mu + \mu_1) \cdot \cos\beta \cdot \sum_{k=1}^{n_a} W_{(k)} \end{aligned} \tag{29}$$

where $\boldsymbol{n_a}$ is the number of packages being accumulated and $\boldsymbol{\mu_1}$ is the friction coefficient between belt and the accumulated material. Similar to the expression for conveying, Eq. (29) can be rewritten as:

$$F_{fa} = (\mu + \mu_1) \cdot w_{ma} \cdot L_a \cos\beta \tag{30}$$

where $\boldsymbol{w_{ma}}$ is weight distribution over a unit of accumulation length and $\boldsymbol{L_a}$ is the accumulation length.

The gravitational load, $\boldsymbol{F_g}$, is the component of material weight parallel to the belt

$$F_g = \sin\beta \cdot \sum_{k=1}^{n_c + n_a} W_{(k)} \tag{31}$$

Note that the Eq. (31) can be also expressed as

$$F_g = (w_m \cdot L_m + w_{ma} \cdot L_a) \cdot \sin\beta \tag{32}$$

In *vacuum conveyors* (Fig. 7) normally, the main resistance to the motion (thus the main component of the effective tension) consists of the friction force $\boldsymbol{F_{fv}}$ created by the vacuum between the belt and slider bed. $\boldsymbol{F_{fv}}$ is given by

$$F_{fv} = \mu \cdot P \cdot A_v \tag{33}$$

where $\boldsymbol{P}$ is the magnitude of the vacuum pressure relative to the atmospheric pressure and $\boldsymbol{A_v}$ is the total area of the vacuum openings in the slider bed. A uniformly distributed pressure accounts for a linear increase of the tight side tension as depicted in Fig. 7.

Shaft forces

Force equilibrium at the driver or driven pulley yields relationships between tight and slack side tensions and the shaft reaction forces $\boldsymbol{F_{s1}}$ or $\boldsymbol{F_{s2}}$. In power transmission drives (see Fig. 3) the forces on both shafts are equal in magnitude and are given by

$$F_{s1,2} = \sqrt{T_1^2 + T_2^2 - 2 \cdot T_1 \cdot T_2 \cdot \cos\theta_1} \quad (34)$$

where $\boldsymbol{\theta_1}$ is angle of belt wrap around driver pulley.
Note that unlike power transmission drives, both linear positioners (Fig 4) and conveyors (Figs. 6 and 7) have no driven pulley - the second pulley is an idler.

In conveyor and linear positioner drives the shaft force at the driver pulley, F_{s1}, is given by

$$F_{s1} = \sqrt{T_1^2 + T_2^2 - 2 \cdot T_1 \cdot T_2 \cdot \cos\theta_1} \quad (35)$$

when $\theta_1 \neq \theta_2 \neq 180^\circ$ (unequal pulley diameters) and by

$$F_{s1} = T_1 + T_2 \quad (36)$$

when $\theta_1 = \theta_2 = 180^\circ$ (equal pulley diameters), where $\boldsymbol{\theta_2}$ is angle of belt wrap around idler pulley.

The shaft force at the idler pulley, $\boldsymbol{F_{s2}}$, when the load (conveyed material or slider) is moving toward the driver pulley is given by

$$F_{s2} = \sqrt{T_2^2 + T_2''^2 - 2 \cdot T_2 \cdot T_2'' \cdot \cos\theta_2} \quad (37)$$

when $\theta_1 \neq \theta_2 \neq 180^\circ$ or by

$$F_{s2} = T_2 + T_2'' \quad (38)$$

when $\theta_1 = \theta_2 = 180^\circ$. T_2'' is given by

$$T_2'' = T_2 + F_{ai} \quad (39)$$

where $\boldsymbol{F_{ai}}$ is given by Eq. (21).

However, when the load is moving away from the driver pulley the shaft force at the idler pulley, $\boldsymbol{F_{s2}}$, is given by

$$F_{s2} = \sqrt{T_1^2 + T_1'^2 - 2 \cdot T_1 \cdot T_1' \cdot \cos\theta_1} \quad (40)$$

when $\theta_1 \neq \theta_2 \neq 180^\circ$ or by

$$F_{s2} = T_1 + T_1' \quad (41)$$

when $\theta_1 = \theta_2 = 180^\circ$. T_1' is given by

$$T_1' = T_1 - F_{ai} \quad (42)$$

Eqs. (39) and (42) assume no friction in the bearings supporting the idler pulley. Observe that during constant velocity motion Eq. (38) can be expressed as

$$F_{s2} = 2 \cdot T_2 \quad (43)$$

The same applies to Eq. (41).

In linear positioning drives such as "configuration II" (shown in Fig. 5) the shaft force of the driver pulley, $\boldsymbol{F_{s1}}$, is given by Eq. (35). The shaft forces on the idler rollers can be expressed by

$$\begin{aligned} F_{s2}' &= \sqrt{T_1^2 + T_1'^2 - 2 \cdot T_1 \cdot T_1' \cdot \cos\theta_2'} \\ F_{s1}'' &= \sqrt{T_2^2 + T_2''^2 - 2 \cdot T_2 \cdot T_2'' \cdot \cos\theta_2''} \end{aligned} \quad (44)$$

where F_{s2}' is the shaft force at the idler on the side of the tight side tension, θ_2' is the angle of belt wrap around the idler pulley on the side of the tight side tension, F_{s2}'' is the shaft force at the idler on the side of the slack side tension and θ_2'' is the angle of belt wrap around the idler pulley on the side of the slack side tension. Tension forces $T_1^{'}$ and $T_2^{''}$ are given by Eqs. (39) and (42).

In the drive shown in Fig. 5 $\theta_1 = 180°$ and $\theta_2^{'} = \theta_2^{''} = 90°$, and the shaft force at the driver pulley is given by Eq. (36) and the shaft forces at the idler rollers become

$$F_{s2}^{'} = \sqrt{T_1^2 + T_1^{'2}}$$
$$F_{s2}^{''} = \sqrt{T_2^2 + T_2^{''2}} \tag{45}$$

Observe that in reversing drives (like linear positioners in Fig. 4) the shaft force at the idler pulley, $\boldsymbol{F_{s2}}$, changes depending on the direction of rotation of the driver pulley. For the same operating conditions $\boldsymbol{F_{s2}}$ is larger when the slider moves away from the driver pulley.

To determine tight and slack side tensions as well as the shaft forces (2 equations with 3 unknowns), given either the torque $\boldsymbol{M}$ or the effective tension $\boldsymbol{T_e}$, an additional equation is still required. This equation will be obtained from analysis of belt pre-tension methods presented in the next section.

Belt Pre-tension

The *pre-tension*, $\boldsymbol{T_i}$, (sometimes referred to as *initial tension*) is the belt tension in an idle drive (Fig. 8). When belt drive operates under load tight side and slack sides develop. The pre-tension prevents the slack side from sagging and ensures proper tooth meshing. In most cases, timing belts perform best when the magnitude of the slack side tension, $\boldsymbol{T_2}$, is 10% to 30% of the magnitude of the effective tension, $\boldsymbol{T_e}$

$$T_2 \in (0.1,\ldots,0.3) \cdot T_e \tag{46}$$

In order to determine the necessary pre-tension we need to examine a particular drive configuration, loading conditions and the pre-tensioning method.

To pre-tension a belt properly, an adjustable pulley or idler is required (Figs. 3, 4, 6 and 7). In linear positioners where open-ended belts are used (Figs. 4 and 5) the pre-tension can also be attained by tensioning the ends of the belt. In Figs. 3 to 7 the amount of initial tension is graphically shown as the distance between the belt and the dashed line.

Although generally not recommended, a configuration without a mechanism for adjusting the pre-tension may be implemented. In this type of design, the center distance has to be determined in a way that will ensure an adequate pre-tension after the belt is installed. This method is possible because after the initial tensioning and straightening of the belt, there is practically no post-elongation (creep) of the belt. Consideration must be given to belt elasticity, stiffness of the structure and drive tolerances.

Drives with a fixed center distance are attained by locking the position of the adjustable shaft after pre-tensioning the belt (Figs. 3, 4, 6 and 7). The overall belt length remains constant during drive operation regardless of the loading conditions (belt sag and some other minor influences are neglected). The reaction force on the locked shaft generally changes under load. We will show later that the slack and tight side tensions depend not only on the load and the pre-tension, but also on the belt elasticity. Drives with a fixed center distance are used in linear positioning, conveying and power transmission applications.

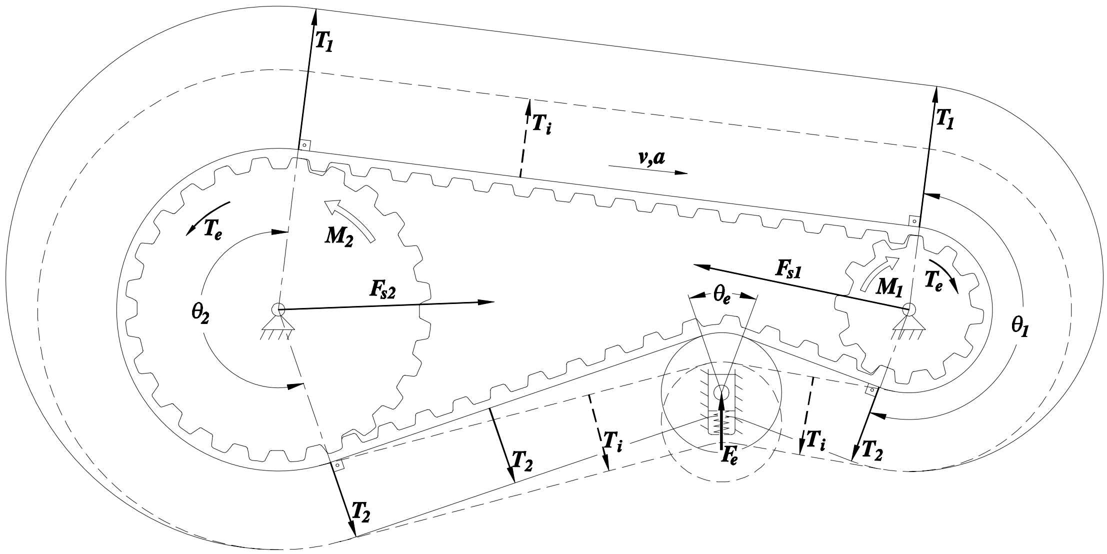

Figure 9. Power transmission drive with the constant slack side tension.

Drives with a constant slack side tension have an adjustable idler tensioning the slack side which is *not locked* (floating) (Figs. 9 and 10). During operation, the consistency of the slack side tension is maintained by the external tensioning force, $\boldsymbol{F_e}$. The length increase of the tight side is compensated by a displacement of the idler. Drives with a constant slack side tension may be considered for some conveying applications.

Resolving the Tension Forces

Drives with a constant slack side tension have an external load system, which can be determined from force analysis alone. Force equilibrium at the idler gives

$$T_i \approx T_2 = \frac{F_e}{2 \cdot \sin\left(\frac{\theta_e}{2}\right)} \tag{47}$$

where $\boldsymbol{F_e}$ is the external tensioning force and θ_e is the wrap angle of the belt around the idler (Figs. 9 and 10).
Eq. (47) together with Eq. (11) can be used to solve for the tight side tension, $\boldsymbol{T_1}$, as well as the shaft reactions, $\boldsymbol{F_{s1}}$ and $\boldsymbol{F_{s2}}$.
Drives with a fixed center distance (Figs. 3, 4, 6 and 7) have an external load system, which cannot be determined from

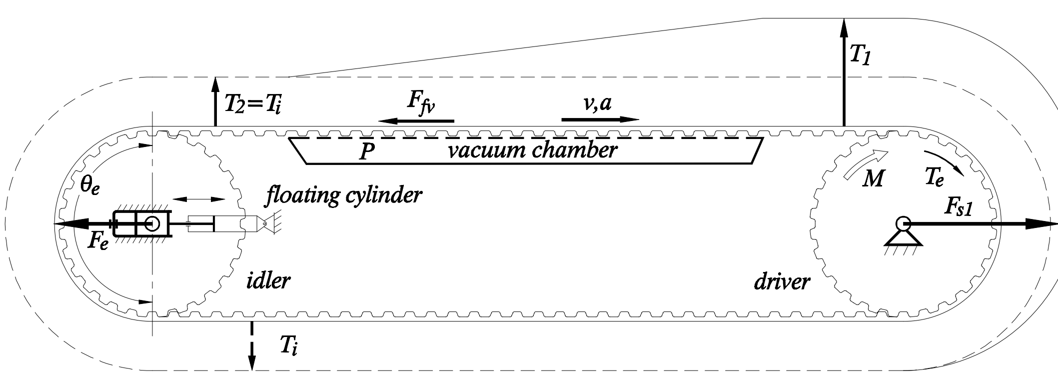

Figure 10. Vacuum conveyor with the constant slack side tension.

force analysis alone. To calculate the belt tension forces, T_1 and T_2, an additional relationship is required. This relationship can be derived from belt elongation analysis. Pulleys, shafts and mounting structures are assumed to have infinite rigidity. Neglecting the belt sag as well as some phenomena with little contribution (such as bending resistance of the belt and radial shifting of the pitch line explained later), the total elongation (deformation) of the belt operating under load is equal to the total belt elongation resulting from the belt pre-tension. This can be expressed by the following equation of geometric compatibility of deformation:

$$\Delta L_{11} + \Delta L_{22} + \Delta L_{me} = \Delta L_{1i} + \Delta L_{2i} + \Delta L_{mi} \tag{48}$$

where ΔL_{11} and ΔL_{22} are tight and slack side elongation due to T_1 and T_2, respectively, ΔL_{me} is the total elongation of the belt portion meshing with the driver (and driven) pulley, ΔL_{1i}, ΔL_{2i} and ΔL_{mi} are the respective deformations caused by the belt pre-tension, T_i.

For most practical cases the difference between the deformations of the belt in contact with both pulleys during pre-tension and during operation is negligible ($\Delta L_{me} \approx \Delta L_{mi}$). Eq. (48) can be simplified

$$\Delta L_{11} + \Delta L_{22} = \Delta L_{1i} + \Delta L_{2i} \tag{49}$$

Tensile tests show that in the tension range timing belts are used, stress is proportional to strain. Defining the stiffness of a unit long and a unit wide belt as *specific stiffness*, c_{sp}, the *stiffness coefficients* of the belt on the tight and slack side, k_1 and k_2, are expressed by

$$k_1 = c_{sp} \cdot \frac{b}{L_1} \qquad k_2 = c_{sp} \cdot \frac{b}{L_2} \tag{50}$$

where L_1 and L_2 are the *unstretched lengths* of the tight and slack sides, respectively, and b is the *belt width*. Note that the expressions in Eq. (50) have a similar form to the formulation for the axial stiffness of a bar $k = E \cdot \frac{A}{l}$ where E is Young's modulus, A is cross sectional area and l is the length of the bar.

It is known that elongation equals tension divided by stiffness coefficient, $\Delta L = \frac{T}{k}$, provided the tension force is constant over the belt length. Thus, Eq. (49) can be expressed as

$$\frac{T_1}{k_1} + \frac{T_2}{k_2} = \frac{T_i}{k_1} + \frac{T_i}{k_2} \tag{51}$$

Combining expressions for the stiffness coefficients, Eq. (50) with Eq. (51) the tight and slack side tensions, T_1 and T_2, are given by

$$T_1 = T_i + T_e \frac{L_2}{L_1 + L_2} = T_i + T_e \frac{L_2}{L} \tag{52}$$

and

$$T_2 = T_i - T_e \frac{L_1}{L_1 + L_2} = T_i - T_e \frac{L_1}{L} \tag{53}$$

where L is the total belt length, L_1 and L_2 are the lengths of the tight and slack sides respectively. Using Eqs. (52) and (53) we can find the shaft reaction forces, F_{s1} and F_{s2}.

In practice, a belt drive can be designed such that the desired slack side tension, T_2, is equal to 10% to 30% of the effective tension, T_e (see Eq. (46)), which secures proper tooth meshing during belt drive operation. Then Eq. (53) can be used to calculate the pre-tension ensuring that the slack side tension is within the recommended range.

As mentioned before, Eqs. (51) through (53) apply when tight and slack side tensions are constant over the length. In all other cases the elongation in Eq. (49) must be calculated according to the actual tension distribution. For example, the elongation of the conveying length L_v over the vacuum chamber length presented in Fig. 7, caused by a linearly increasing belt tension, equals the mean tension, $\hat{T}$, where $\hat{T} = \frac{T_1 + T_2}{2}$, divided by the stiffness k_v where $k_v = c_{sp}\frac{b}{L_v}$ of this belt portion, b is the belt width, L_v is the length of the vacuum chamber T_1 and T_2 are the tensions at the beginning and end of the vacuum chamber stretch, respectively. Considering this, T_1 and T_2 can be expressed by

$$T_{1\,max} = T_i + T_e \frac{L_2 + \frac{L_v}{2}}{L} \quad (54)$$

$$T_{2\,min} = T_i - T_e \frac{L_1 + \frac{L_v}{2}}{L} \quad (55)$$

Substituting $L_1^* = L_1 + \frac{L_v}{2}$ and $L_2^* = L_2 + \frac{L_v}{2}$ Eqs. (54) and (55) can be expressed in the form of Eqs. (52) and (53), respectively.

A similar analysis can be performed for the conveyor drive in Fig. 6, with the belt elongation due to the mean tension

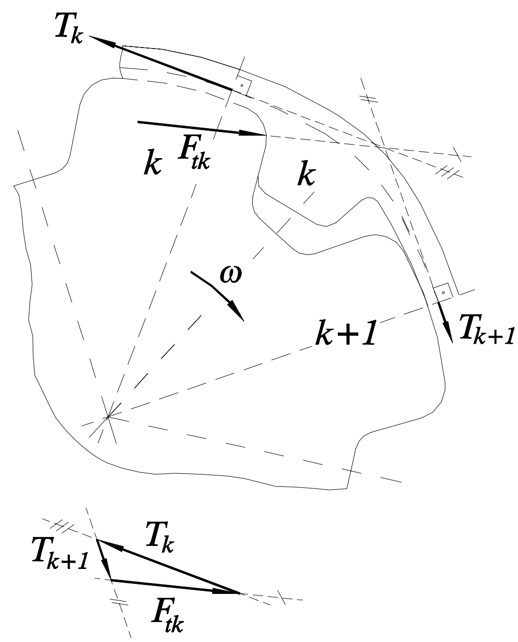

Figure 11. Tooth loading.

calculated over the conveying and accumulation length, $L_m + L_a$. The distance, $\hat{L}$ ($0 < \hat{L} < L_m + L_a$), from the beginning of the conveying length to the location on the belt corresponding to the mean tension, $\hat{T}$, should be calculated. The modified tight and slack lengths take on the following form:

$$\begin{aligned} L_1^* &= L_1 + L_m + L_a - \hat{L} \\ L_2^* &= L_2 + \hat{L} \end{aligned} \quad (56)$$

Tooth Loading

Consider the belt in contact with the driver pulleys in belt drives presented in (Figs. 3 to 10). Starting at the tight side, the belt tension along the arc of contact decreases with every belt tooth. At the k[th] tooth, the tension forces T_k and T_{k+1} are balanced by the force F_{tk} at the *tooth flank* (Fig. 11). The force equilibrium can be written as

$$\vec{T}_k + \vec{T}_{k+1} + \vec{F}_{tk} = 0 \quad (57)$$

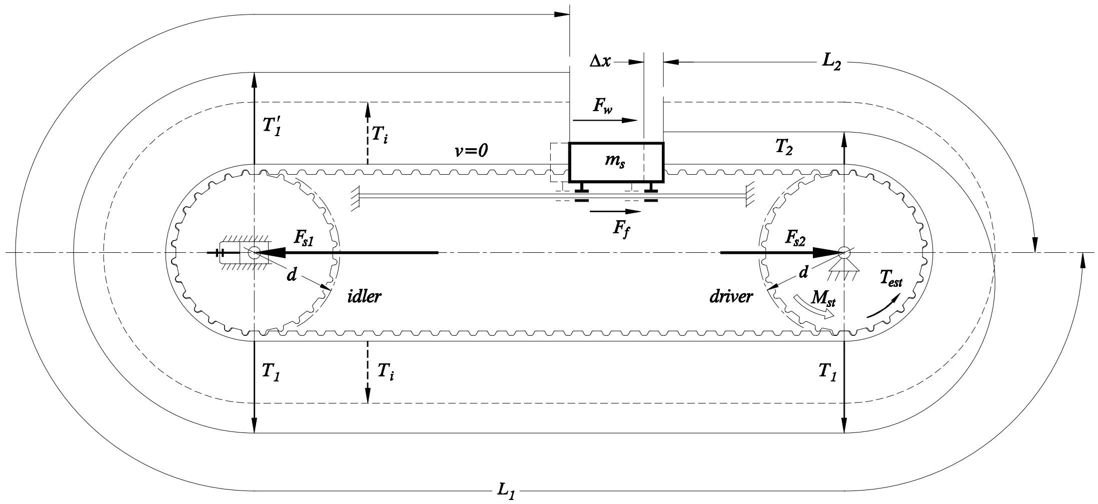

Figure 12. Position error - linear positioner under static loading condition.

In order to fulfill the equilibrium conditions, the belt tooth inclines and moves radially outwards as shown in Fig. 11. In addition to tooth deformation, tooth shifting contributes to the relative displacement between belt and pulley, hence to the tooth stiffness.

Theoretically, the tooth stiffness increases with increasing belt tension over the tooth, which has also been confirmed empirically. This results in the practical recommendation for linear actuators to operate under high pre-tension in order to achieve higher stiffness, and hence, better positioning accuracy. However, to simplify the calculations, a constant value for the *tooth stiffness*, $\boldsymbol{k_t}$, is used in the formulas presented in the next section.

Positioning Error of Timing Belt Drives Due to Belt Elasticity

To determine the positioning error of a linear actuator, caused by an external force at the slide, the stiffness of tight and slack sides as well as the stiffness of belt teeth and cords along the arc of contact have to be considered. Since tight and slack sides can be considered as springs acting in parallel, their stiffness add linearly to form a *resultant stiffness (spring) constant* $\boldsymbol{k_r}$

$$k_r = k_1 + k_2 = c_s \cdot b \frac{L_1 + L_2}{L_1 \cdot L_2} \qquad (58)$$

In linear positioners (Figs. 12 and 13), the length of tight and slack side and therefore the resultant spring constant depend on the position of the slide. The resultant stiffness exhibits a minimum value at the position where the difference between tight and slack side length is minimum.

To determine the *resultant stiffness of the belt teeth and cords in the teeth-in-mesh area,* $\boldsymbol{k_m}$, observe that the belt teeth are deformed non-uniformly and act in a parallel like arrangement with reinforcing cord sections, but the belt sections between them are connected in series. The solution to the problem is involved and beyond the scope of this paper but the result is presented in Graph 1. The ordinate is made dimensionless by dividing $\boldsymbol{k_m}$ by the tooth stiffness $\boldsymbol{k_t}$. Graph 1 shows that the gradient of $\boldsymbol{k_m}$ (indicated by the slope of the curve) decreases with increasing number of teeth in mesh.

Defining the ratio $\frac{k_m}{k_t}$ as the *virtual number of teeth in mesh*, $\boldsymbol{z_{mv}}$, corresponding to the *actual number of teeth in mesh* $\boldsymbol{z_m}$ the stiffness of the belt and the belt teeth around the arc of contact is

$$k_m = z_{mv} \cdot k_t \tag{59}$$

Observe that the virtual number of teeth in mesh, $\boldsymbol{z_{mv}}$, remains constant and equals 15 for the actual number of belt teeth in mesh $\boldsymbol{z_m} \geq 15$. The result of this is that the maximum number of teeth in mesh that carry load is 15.

In linear positioners the displacement of the slide due to the elasticity of the tight and slack sides has to be added to the displacement due to the elasticity of the belt teeth and cords in the teeth-in-mesh area. Therefore, the *total drive stiffness*, $\boldsymbol{k}$, is determined by the following formula:

$$\frac{1}{k} = \frac{1}{k_r} + \frac{1}{k_m} \tag{60}$$

In drives with a driven pulley (power transmission drives) an additional term: $\frac{1}{k_{m2}}$ must be added to the right-hand side of Eq. (60). This term introduces the stiffness of the belt and belt teeth around the driven pulley.

The *static positioning error*, $\boldsymbol{\Delta x}$ of a linear positioner due to the elasticity of the belt cords and teeth is

$$\Delta x = \frac{F_{st}}{k} \tag{61}$$

where $\boldsymbol{F_{st}}$ is the static (external) force remaining at the slide. In Fig. 12, for example, $\boldsymbol{F_{st}}$ is comprised of $\boldsymbol{F_f}$ and $\boldsymbol{F_w}$, and it is balanced by the static effective tension $\boldsymbol{T_{est}}$ at the driver pulley.
The additional rotation angle, $\boldsymbol{\Delta\varphi}$, of the driving pulley necessary for exact positioning of the slide is

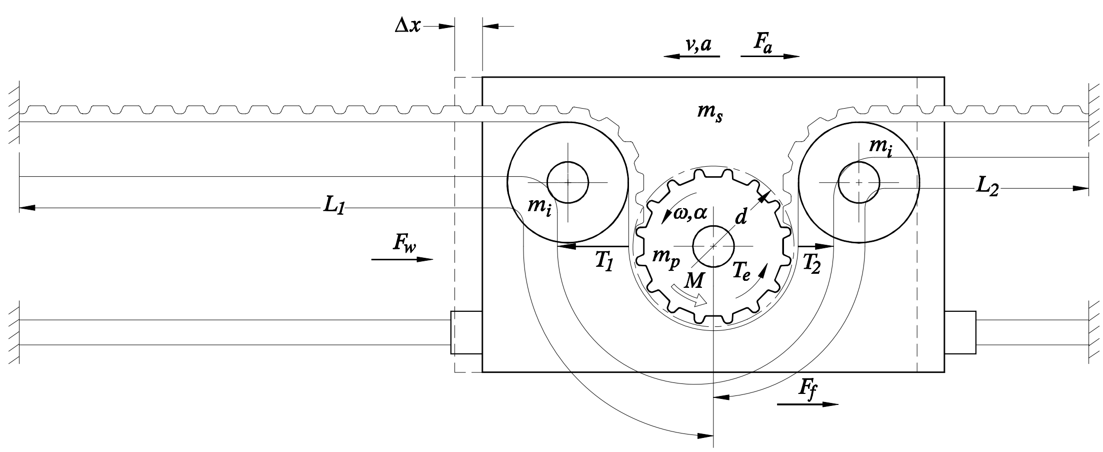

Figure 13. Following error - linear positioner under dynamic loading condition.

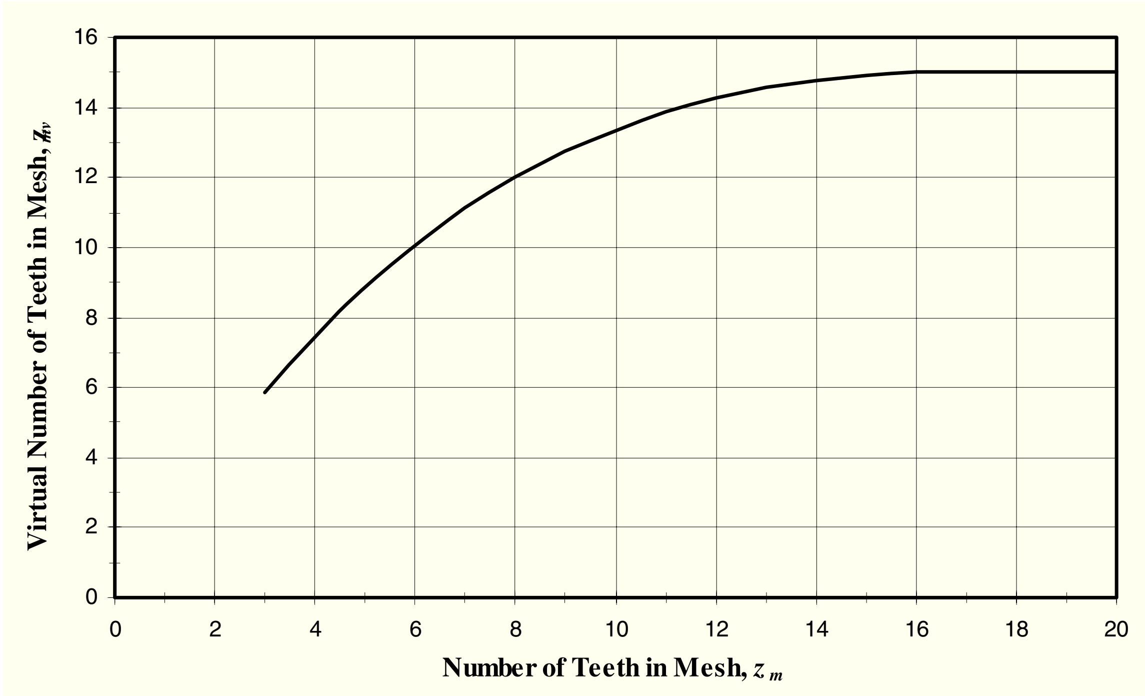

Graph 1. Correction for the number of teeth in mesh (virtual # of teeth in mesh vs. actual # of teeth in mesh)

$$\Delta\varphi = \frac{M}{k_\varphi} = \frac{T_{est}}{\frac{d}{2} \cdot k} \qquad (62)$$

Substituting ***M*** from Eq. (12) in Eq. (62) the relationship between *linear stiffness,* ***k***, and *rotational stiffness*, $\boldsymbol{k_\varphi}$, can be obtained

$$k_\varphi = \frac{d^2 \cdot k}{4} \qquad (63)$$

Observe that using pulleys with a larger pitch diameter increases the rotational stiffness of the drive, but also increases the torque on the pulley shaft and the inertia of the pulley.

Metric AT series belts have been designed for high performance linear positioner applications. Utilizing optimized, larger tooth section and stronger steel reinforcing tension members these belts provide a significant increase in tooth stiffness and overall belt stiffness.

A Tomkins Company

GATES MECTROL, INC.
9 Northwestern Drive
Salem, NH 03079, U.S.A.
Tel. +1 (603) 890-1515
Tel. +1 (800) 394-4844
Fax +1 (603) 890-1616
email: apps@gatesmectrol.com

GM_Belt Theory_06_US